Japanese Journal of Applied Physics **54**, 08KA12 (2015) **REGULAR PAPER**
http://dx.doi.org/10.7567/JJAP.54.08KA12

MOVPE growth of thick (~1 μm) InGaN on AlN/Si substrates for InGaN/Si tandem solar cells

Akio Yamamoto[1,2], Kazuki Kodama[1], Md. Tanvir Hasan[1,2], Naoteru Shigekawa[3], and Masaaki Kuzuhara[1]

[1]*University of Fukui, Fukui 910-8507, Japan*
[2]*JST-CREST, Chiyoda, Tokyo 102-0076, Japan*
[3]*Osaka City University, Osaka 558-8585, Japan*

Received January 24, 2015; accepted May 11, 2015; published online July 21, 2015

In order to develop key technologies for InGaN/Si two-junction tandem solar cells, MOVPE growth of thick InGaN on Si p-on-n cell structures has been studied. By clarifying the phase separation behavior of MOVPE InGaN, a thick (~1 μm) $In_xGa_{1-x}N$ ($x \sim 0.5$) without phase separation is successfully grown on AlN/Si(111) wafers. A sufficient current flow for the operation of the tandem cell is obtained through n-InGaN/AlN/p-Si structures by employing the annealing of AlN/Si wafer at around 1000 °C in NH_3 flow just before InGaN growth. The annealing of AlN/Si wafers also brings about the degradation of the underlying Si pn junction. The optimization of the annealing conditions is required to balance such favorable and unfavorable effects.

1. Introduction

InGaN compound semiconductors have been predicted as excellent candidates for full-solar spectrum photovoltaic (PV) applications,[1,2] because of their tunable band gap in the wide range of 0.7–3.4 eV. As InGaN-based solar cells, hetero-junction solar cells with single- or multi-quantum well (QW) structures have been extensively studied.[3] However, their performances have been still poor. One of reasons for this may be insufficient absorption of photons in thin InGaN well (absorption) layers. Thickness of absorption layer is one of the critical parameters in solar cells. In the case of incident photons for which absorption coefficient is $10^4\,cm^{-1}$, for example, thickness of absorption layer should be 1 μm or more in order to absorb almost of them. Such a thick absorption layer cannot be realized in QW structure cells due to the restriction of the critical thickness for lattice relaxation.[4] A high electric field induced in the InGaN well layer by the piezo polarization also can suppress the carrier extraction from the well region.[5] On the other hand, homo-junction solar cells are free from both the critical thickness issue and the piezo polarization effects. Therefore, homo-junction InGaN solar cell should be more promising as a high efficiency solar cell. Compared with hetero-junction solar cells, however, InGaN homo-junction cells have not been so extensively studied.[3] This is due to the difficulties in growing thick and InN-rich InGaN films. Thus, the growth of thick InGaN films is a very important issue to realize a high efficiency InGaN-based solar cell.

From the practical viewpoint, the combination of $In_{0.45}Ga_{0.55}N$ ($E_g \sim 1.8$ eV) and Si (1.1 eV) is expected to provide a high efficiency two-junction tandem solar cell. Current matching is achieved between the $In_{0.45}Ga_{0.55}N$ top cell and the Si bottom cell, if all photons with an energy higher than 1.8 eV are absorbed in the InGaN top cell. A power conversion efficiency more than 30% is predicted for such an InGaN/Si tandem cell.[6] In addition, it is expected that electrons in the n-InGaN and holes in the p-Si can be easily recombined at the interface (ohmic behavior),[7] indicating that no additional tunnel junction is required to connect the top and the bottom cells. Thus, the InGaN/Si two-junction tandem cell is a very promising approach to effectively increase efficiency of single-crystalline Si solar cells. However, there are many challenges in the fabrication of InGaN/Si 2-junction tandem cell. The major one is the growth of thick $In_xGa_{1-x}N$ ($x \sim 0.5$). In this paper, we have studied the MOVPE growth of thick $In_xGa_{1-x}N$ ($x = 0.2$–0.5) on Si(111) p-on-n cell structures as a key technology for the fabrication of the InGaN/Si tandem cells. The main issue in this topic is how to avoid phase separation in grown InGaN.

In the case of MOVPE growth of III–nitride materials on Si, it is known that the use of an interlayer is inevitable to suppress the nitridation[8] and/or melt-back[9] of Si surface. AlN[10] and/or AlGaN[11] have been widely studied as an interlayer. When such an interlayer is introduced to the InGaN growth, the direct contact of InGaN to Si cannot be realized. As described below, a 100-nm-thick AlN is used as an interlayer in this study. Therefore, the current flow between n-InGaN and p-Si through the AlN interlayer is also studied. Problems related to the deterioration of Si p-on-n cell through the InGaN growth process are also discussed in this paper.

2. Experimental procedure

The growth of InGaN has been carried out using an MOVPE system with a horizontal reactor in the temperature range of 570–750 °C at a pressure of 150 Torr. As sources, trimethylindium (TMI), triethylgallium (TEG), and ammonia (NH_3) are used. An n-type Si(111) with a p layer on the surface is used as a substrate. The p layer is formed by the B ion implantation [50–10 keV, $(7–1) \times 10^{12}/cm^2$] into n-type Si(111) substrate followed by the rapid thermal annealing (RTA) at 1000 °C. A 100-nm-thick AlN layer grown at 1100 °C is used as an interlayer. As a pretreatment of AlN/Si wafers, they are annealed in NH_3 flow at 800–1000 °C for 10–30 min just before InGaN growth. AlN/p-Si(111), GaN/α-Al_2O_3(0001) template and α-Al_2O_3(0001) are also employed as substrates for comparison. The composition of grown films is determined by using X-ray diffraction ($2\theta/\omega$) patterns. As ohmic contacts to n-InGaN, p-Si and n-Si, Au (60 nm thick), Al (60 nm thick), and Au (50 nm thick)/Ni (20 nm thick) are vacuum-evaporated, respectively, and then annealed in N_2 atmosphere at 500 °C for 5 min. Current–voltage (I–V) characteristics for n-InGaN/AlN/p-Si and n-InGaN/AlN/pn-Si structures are measured.

3. Results and discussion

3.1 Preparation of thick (~1 μm) $In_xGa_{1-x}N$ without phase separation

By employing an AlN interlayer, epitaxial InGaN layers are

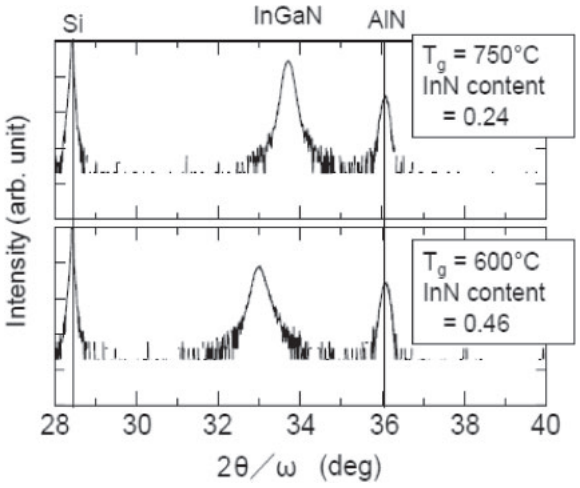

Fig. 1. X-ray $2\theta/\omega$ diffraction profiles for InGaN films with a different InN content grown on AlN/Si(111) substrates.

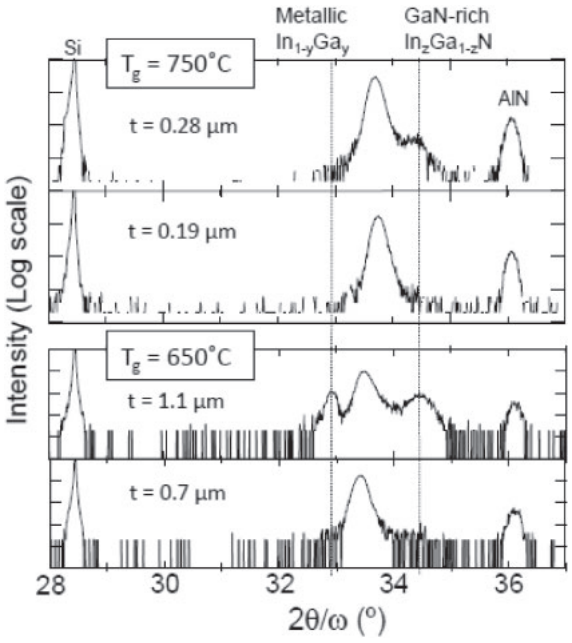

Fig. 2. X-ray $2\theta/\omega$ diffraction profiles for InGaN films with a different thickness grown at 750 and 650 °C. t is thickness of InGaN film.

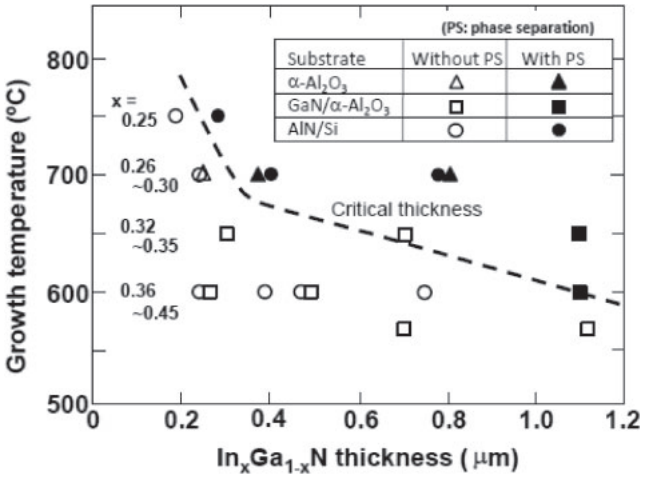

Fig. 3. Mapping of InGaN films with and without phase separation, displayed on the plane of film thickness and growth temperature. The dotted line shows critical thicknesses for phase separation at different growth temperatures.

successfully grown on Si(111). Figure 1 shows the X-ray $2\theta/\omega$ diffraction profiles for InGaN films with a different InN composition. As reported previously,[12] InN composition in grown InGaN films is controlled by not only TMI/(TMI + TEG) molar ratio in the vapor but also growth temperature. The results in the figure shows that single-phase InGaN layers with a different InN composition are successfully obtained by changing growth temperature. Recently, we have studied the phase separation behavior of MOVPE $In_xGa_{1-x}N$ ($x = 0.2$–0.4) grown on AlN/Si substrates.[13] Figure 2 shows the X-ray $2\theta/\omega$ diffraction profiles for InGaN films with a different thickness grown at 650 and 750 °C. The typical feature of a phase-separated InGaN is the simultaneous emergence of both metallic In–Ga and GaN-rich InGaN.[13] In the case for films grown at 650 °C, a film with a thickness of 0.7 μm shows no phase separation, while a film grown at 750 °C shows phase separation when its thickness is less than 0.3 μm. The reason why the metallic In–Ga is scarcely observed in the film grown 750 °C is the evaporation of metallic In from the film due to the high growth temperature. Thus, one can see that phase separation occurs when InGaN thickness exceeds a critical value. In Fig. 3, InGaN films with and without phase separation are mapped on the plane of film thickness and growth temperature. The dotted line, drawn between samples with and without phase separation, shows critical thicknesses for phase separation at different growth temperatures.[14] Critical thickness for phase separation in InGaN is markedly decreased with increasing growth temperature. Because phase separation seems to be caused by the solid-state diffusion of constitutional atoms and its rate seems to be governed by diffusion mobility of constitutional atoms, a smaller critical thickness at a higher temperature shows a larger diffusion mobility of constitutional atoms. No marked differences are found in critical thicknesses among AlN/Si(111), α-Al_2O_3(0001), and GaN/α-Al_2O_3(0001) substrates. From the results in Fig. 3, one can see that growth temperature should be reduced to $\lesssim$600 °C to get a film with a thickness $\gtrsim$1 μm.

3.2 Electrical properties of n-InGaN/AlN/p-Si and n-InGaN/AlN/pn-Si structures

Samples with n-InGaN/AlN/p-Si and n-InGaN/AlN/pn-Si structures are prepared and their electrical properties are measured. The thickness of n-InGaN is about 0.5 μm. In the case of n-InGaN/AlN/p-Si structures, AlN/Si wafers are annealed in NH_3 flow at 1000 °C for 15 min just before InGaN growth. As reported previously,[15] such a annealing just before the growth of InN is effective to suppress metallic In droplet formation on AlN/Si substrates. Therefore, similar pretreatment of AlN/Si wafers is adopted in this study. Figure 4 shows the schematic cross-sectional view of the sample (a) and the I–V curves in the dark (b) for n-InGaN/AlN/p-Si structures. The InN content in InGaN layer is varied from 0.14 to 0.49. Surprisingly, all the samples show good ohmic characteristics in spite of the presence of the AlN interlayer, as seen in Fig. 4(b). The resistances obtained from a slope of the I–V curves are found to be markedly reduced with increasing InN content. Such results are very interesting

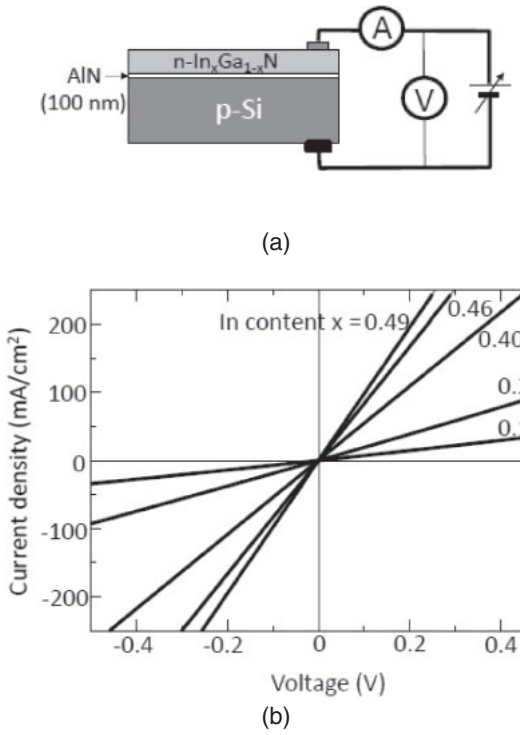

Fig. 4. (a) Schematic drawing of the device structure and (b) *I–V* characteristics for n-InGaN/AlN/p-Si structures with different annealing conditions of AlN/p-Si wafers just before InGaN growth.

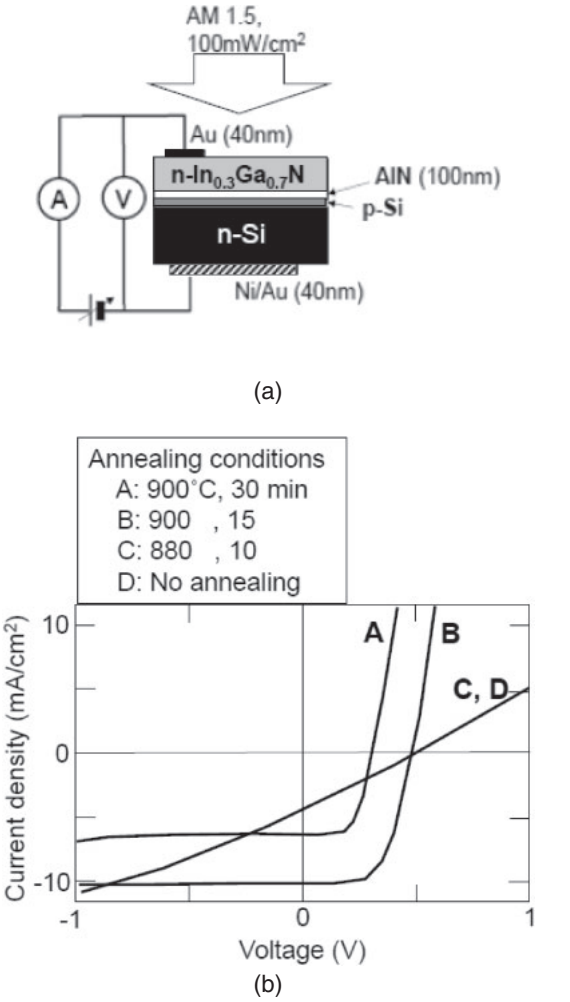

Fig. 5. (a) Schematic drawing of the device structure and (b) *I–V* characteristics for n-InGaN/AlN/pn-Si structures with different annealing conditions of AlN/pn-Si wafers just before InGaN growth.

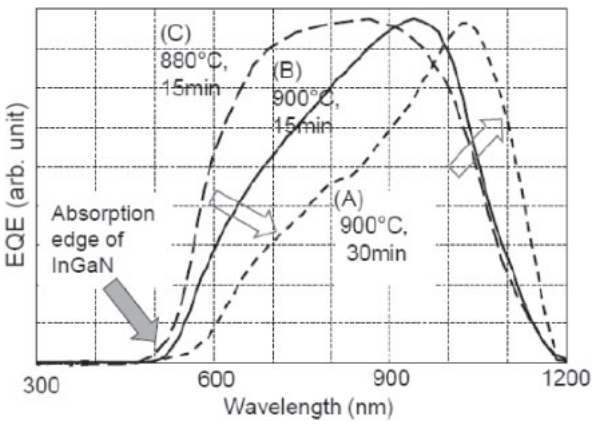

Fig. 6. Spectral response for Si cells with different annealing conditions for AlN/pn-Si wafers just before InGaN growth.

and useful for the device application of the n-InGaN/p-Si structure. For example, a resistance as low as $1\,\Omega\,cm^2$ for a film with InN content 0.5 will give no significant effects to the series resistance of InGaN/Si tandem cell. However, the results shown in Fig. 4(b) cannot be easily understood, because a 100-nm-thick AlN interlayer exists between the epilayer and the substrate, and the AlN layer seems to be insulating.

As discussed above, the annealing of AlN/Si wafer at 1000 °C just before InGaN growth brings about the good ohmic characteristics for n-InGaN/AlN/p-Si systems. Here, photovoltaic characteristics of Si p-on-n cells are studied using n-InGaN/AlN/pn-Si structures with different annealing conditions. Since a Si p-on-n cell structure annealed at 1000 °C shows severely deteriorated performance, annealing temperature for AlN/pn-Si is reduced to around 900 °C. Even such a low-temperature annealing brings about the good ohmic characteristics for n-InGaN/AlN/p-Si systems. The *I–V* characteristics for n-InGaN/AlN/pn-Si structures are shown in Fig. 5. The annealing at 880–900 °C has also favorable effects: marked reduction of series resistance R_s and increase in fill factor. The series resistance (R_s) for samples C and D is on the level of $100\,\Omega\,cm^2$, while it is around $5\,\Omega\,cm^2$ for samples A and B. Thus, a sufficient current flow for the operation of the tandem cell is obtained through the n-InGaN/AlN/p-Si structure. The marked increase in fill factor for samples A and B is also due to the reduced R_s. When temperature and time for the annealing are increased, degradation of the Si pn junction, such as decrease of open-circuit voltage (V_{oc}) and short-circuit current density (J_{sc}), are observed. Provided that R_s is determined by the resistance of the AlN interlayer, the resistivity of AlN layer can be estimated to be 10^5–$10^6\,\Omega\,cm$ for the samples C and D. A similar resistivity value was reported for AlN layers containing C and O.[16)]

As seen in Fig. 5, the annealing at 900 °C for 30 min results in the decrease of V_{oc}, indicating some degradation of the Si pn junction. Similar degradation is also found in the spectral response. Figure 6 shows the spectral response for p-on-n structure Si cells with different annealing conditions

for AlN/Si substrates. The absorption edge of $In_{0.3}Ga_{0.7}N$ is clearly seen at around 500 nm wavelength. One can see that the collection efficiency at a relatively short wavelength region (600–800 nm) is reduced with increasing temperature and time for the annealing. This means the increase in junction depth due to the redistribution of implanted B atoms in Si during the annealing. Thus, the annealing of AlN/Si before InGaN growth brings both favorable and unfavorable effects on the solar properties of the Si cell. Therefore, it is a key issue to optimize the annealing conditions.

As described above, resistivity of the AlN layer on Si is markedly decreased and photovoltaic properties of the pn-Si are changed during the annealing process of AlN/Si at around 900 °C just before InGaN growth. For such marked reduction of resistivity in AlN, not only carbon (C) incorporation[16,17] but also Si diffusion[18,19] into the AlN layer seems to be responsible. On the other hand, the photovoltaic property change seems to be due to the diffusion of implanted B atoms. However, it should be noted that the B-implanted n-Si wafers suffer thermal treatments at a temperature higher than 900 °C; RTA at 1000 °C after B implantation and AlN growth at 1100 °C. Therefore, it can not be easily understood that the annealing process at around 900 °C just before InGaN growth has such significant effects. In order to clarify this, detailed analysis of samples at each stage of the processes, including resistivity measurement for AlN and impurity distribution analysis in AlN and Si, will be needed.

4. Conclusions

In order to realize InGaN homo-junction of Si pn junction, the MOVPE growth of thick InGaN on Si p-on-n structures has been studied using an AlN interlayer. Phase separation behavior of MOVPE InGaN is studied by pay attention to growth temperature and film thickness as main growth parameters. Based on that, a thick (~1 μm) $In_xGa_{1-x}N$ ($x \sim 0.5$) layer without phase separation is successfully grown on Si(111) by reducing growth temperature to $\lesssim$600 °C. A sufficient current flow for the operation of the tandem cell is obtained through n-InGaN/AlN/p-Si structures by employing the annealing of AlN/Si wafers in NH_3 flow just before InGaN growth. In addition to such favorable effects, the annealing of AlN/Si wafers deteriorates the electrical properties of the underlying Si pn junction with increasing temperature and duration for the annealing. Therefore, it is very important to optimize the annealing conditions in order to balance the favorable and unfavorable effects.

Acknowledgement

This work was supported in part by "Creative research for clean energy generation using solar energy" project in CREST programs of JST, Japan.

1) J. Wu, W. Walukiewicz, K. M. Yu, W. Shan, J. W. Ager, III, E. E. Haller, H. Lu, W. J. Schaff, W. K. Metzger, and S. Kurtz, J. Appl. Phys. **94**, 6477 (2003).
2) A. Yamamoto, Md. R. Islam, T.-T. Kang, and A. Hashimoto, Phys. Status Solidi C **7**, 1309 (2010).
3) A. G. Bhuiyan, K. Sugita, A. Hashimoto, and A. Yamamoto, IEEE J. Photovoltaics **2**, 276 (2012).
4) S. Pereira, M. R. Correia, E. Pereira, C. Trager-Cowan, F. Sweeney, K. P. O'Donnell, E. Alves, N. Franco, and A. D. Sequeira, Appl. Phys. Lett. **81**, 1207 (2002).
5) J. J. Wierer, Jr., A. J. Fischer, and D. D. Koleske, Appl. Phys. Lett. **96**, 051107 (2010).
6) L. Hsu and W. Walukiewicz, J. Appl. Phys. **104**, 024507 (2008).
7) J. W. Ager, L. A. Reichertz, K. M. Yu, W. J. Schaff, T. L. Williamson, M. A. Hoffbauer, N. M. Haegel, and W. Walukiewicz, Proc. 33rd IEEE Photovoltaic Specialists Conf., 2008, p. 110.
8) A. Yamamoto, M. Tsujino, M. Ohkubo, and A. Hashimoto, J. Cryst. Growth **137**, 415 (1994).
9) A. Ubukata, K. Ikenaga, N. Akutsu, A. Yamaguchi, K. Matsumoto, T. Yamazaki, and T. Egawa, J. Cryst. Growth **298**, 198 (2007).
10) W. Luo, X. Wang, L. Guo, H. Xiao, C. Wang, J. Ran, J. Li, and J. Li, Microelectron. J. **39**, 1710 (2008).
11) K.-L. Lin, E.-Y. Chang, Y.-L. Hsiao, W.-C. Huang, T.-T. Luong, Y.-Y. Wong, T. Li, D. Tweet, and C.-H. Chiang, J. Vac. Sci. Technol. B **28**, 473 (2010).
12) A. Yamamoto, K. Sugita, A. G. Bhuiyan, A. Hashimoto, and N. Narita, Mater. Renewable Sustainable Energy **2**, 10 (2013).
13) A. Yamamoto, Md. T. Hasan, A. Mihara, N. Narita, N. Shigekawa, and M. Kuzuhara, Appl. Phys. Express **7**, 035502 (2014).
14) A. Yamamoto, T. Md Hasan, K. Kodama, N. Shigekawa, and M. Kuzuhara, J. Cryst. Growth **419**, 64 (2015).
15) A. G. Bhuiyan, A. Mihara, T. Esaki, K. Sugita, A. Hashimoto, A. Yamamoto, N. Watanabe, H. Yokoyama, and N. Shigekawa, Phys. Status Solidi C **9**, 670 (2012).
16) M. Okamoto, Y. K. Yap, M. Yoshimura, Y. Mori, and T. Sasaki, Diamond Relat. Mater. **10**, 1322 (2001).
17) K. Wongchotigul, N. Chen, D. P. Zhang, X. Tang, and M. G. Spencer, Mater. Lett. **26**, 223 (1996).
18) B. S. Zhang, M. Wu, X. M. Shen, J. Chen, J. J. Zhu, J. P. Liu, G. Feng, D. G. Zhao, Y. T. Wang, and H. Yang, J. Cryst. Growth **258**, 34 (2003).
19) G. M. Wu and T. H. Hsieh, J. Achiev. Mater. Manuf. Eng. **24**, 193 (2007).